Accuracy Assessment of ASTER and SRTM DEMs: A Case Study in Andean Patagonia

Mariano F. Gómez[1]
Laboratorio de Geomática. Centro de Investigación y Extensión Forestal Andino Patagónico (CIEFAP), Ruta 259 Km 4, Esquel, Chubut, Argentina

José D. Lencinas
Laboratorio de Geomática. Centro de Investigación y Extensión Forestal Andino Patagónico (CIEFAP) and Universidad Nacional de la Patagonia San Juan Bosco, Ruta 259 Km 4, Esquel, Chubut, Argentina

Antje Siebert and Gastón M. Díaz
Laboratorio de Geomática. Centro de Investigación y Extensión Forestal Andino Patagónico (CIEFAP), Ruta 259 Km 4, Esquel, Chubut, Argentina

Abstract: The ASTER global digital elevation model (GDEM) and the SRTM-C digital elevation model (DEM) provide nearly global coverage, with spatial resolutions of 30 and 90 m, respectively. We assessed the geolocation, elevation, and morphological accuracy of the SRTM-C, the ASTER GDEM, and two single-scene DEMs derived from ASTER data for a site in Patagonia (ASTER DEMs). We found systematic and widely dispersed geolocation errors for the SRTM-C (Linear RMSE = 85.0 m) and the ASTER GDEM (Linear RMSE = 101.1 m). The SRTM-C had a narrow elevation error distribution (RMSE 8.3 ± 2.9 m), whereas the ASTER GDEM had a smaller RMSE (9.4 ± 2.3 m) than the analyzed ASTER DEMs. The ASTER DEMs provided more detailed morphological information than the SRTM-C, but also had more noise.

INTRODUCTION

Natural scientists require information on the shape of the Earth's surface to perform a variety of tasks and applications. In mountainous regions, topographic information is used as a fundamental input when making geometric, radiometric, and atmospheric corrections of satellite imagery obtained from optical and microwave sensor systems (Richter, 2007; Toutin, 2008). This information is also used as ancillary data in image classification processes, especially in regions in which the vegetation distribution is determined by the topographic conditions (Fahsi et al., 1999; Riaño et al., 2003;

---

[1]Corresponding author; email: marianofgomez@gmail.com

Lencinas, 2009). Several attributes derived from digital elevation models (DEMs) in GIS environments are used in geomorphometry (Pike, 2000; Blanchard et al., 2010; Mahmood and Gloaguen, 2011), hydrological modeling (Kenward et al., 2000), and in forecasting tools designed to prevent disasters, such as wildfires (Finney, 1998), or to provide alerts for flood processes (Di et al., 2008; Qi et al., 2009). Depending on the application, topographic data are required to represent either the ground (DEMs) for hydrological and geomorphological applications or the surface of the land cover (digital surface models [DSMs]) for corrections applied to satellite imagery.

Three main sources are used to generate digital elevation models: ground survey techniques, topographic maps, and digital imagery acquired from instruments on airborne or satellite platforms (Nelson et al., 2009). DEMs derived from optical stereo imagery or interferometric synthetic aperture radar (InSAR) techniques are a reliable and cost-effective option for large regions, especially in remote areas and in developing countries. The LiDAR (Airborne Light Detection and Ranging) technology is capable of generating high-precision topographic products, which have been widely developed since the late 90s (Elaksher, 2009). However, there are still regions, especially in developing countries, where its applications are quite limited because of the high costs of the airborne sensor, which depend on the local infrastructure, and the distances to be covered.

The data produced from optical remote sensors, such as the Advanced Spaceborne Thermal Emission and Reflection Radiometer (ASTER), are actually DSMs because these sensors only capture the solar radiation reflected from surfaces through their spectral characteristics (Jacobsen, 2001). Because X-band and C-band are short radar waves, they only slightly penetrate the vegetation. Therefore, the height models derived from the Shuttle Radar Topography Mission (SRTM) are also considered to be DSMs (Sefercik and Jacobsen, 2007). Thus, although most of the widely used datasets are in fact surface models, they are generally referred to as DEMs. For that reason, we will also utilize this nomenclature throughout this paper.

A variety of DEMs available worldwide are generated from both active and passive sensors, are available commercially as well as for free, and have many different spatial resolutions. The SRTM C-band DEM (available free of charge) marked a milestone in the availability of medium- to coarse-resolution elevation data worldwide. It covers approximately 80% of the Earth's land surface and is generated with InSAR techniques from C-band ($\lambda = 5.3$ cm; $f = 5.7$ Ghz) radar data. The product's pixel size is 1 arc second (corresponding to approximately 30 m at the equator) for the territory of the United States and 3 arc seconds (~90 m) for areas outside of the U.S. This DEM is one of the world's most consistent, most complete, and most frequently used environmental datasets (Nelson, 2009). Another sensor on board the same platform, working with X- band ($\lambda = 3.1$ cm; $f = 9.7$ Ghz) microwave signals, provided elevation data with a pixel size of 1 arc second (~30 m). The data products are also available free of charge as 15′ x 15′ tiles, but these tiles cover only certain areas of the globe (Becek, 2008).

Although there are many detailed topographic maps and datasets available at scales of 1:50,000 or larger for some countries, major parts of the Earth are not properly mapped at that scale (Gonçalves and Oliveira, 2004). The launch of ASTER in December 1999 on the Terra platform aims to fill the gap in DEM coverage by providing usable details at a global scale (Toutin, 2008). Its along-track image acquisition

configuration provides a strong advantage in terms of radiometric variations versus multi-date stereo data acquisition with across-track stereo, which may compensate for the weaker stereo geometry (Marangoz et al., 2005). The use of instrument and spacecraft ephemeris information enables one to generate relative DEMs based on ASTER data without field information. These DEMs can be generated via commercial software packages or can be purchased at relatively low cost from the Japanese agency ERSDAC (Earth Remote Sensing Data Analysis Center). These DEMs become "absolute" if ground control points (GCPs) are incorporated into the generation process. In 2009, the Japanese Ministry of Economy, Trade and Industry (METI) and NASA jointly released a global DEM product based on ASTER data. This ASTER Global DEM (ASTER GDEM) has nearly global coverage (83º N to 83º S) and was generated through automated processing of the entire 1.5-million-scene ASTER archive, which produced more than 1,200,000 individual scene-based DEMs (ASTER GDEM Validation Team, 2009). In conjunction with the aforementioned SRTM products, the ASTER data currently provide nearly global coverage at 30 and 90 m spatial resolutions.

In different regions of developing countries with steep relief and extensive, inaccessible regions, such as Patagonia, the lack of accurate, locally derived DEMs was compensated for through the use of SRTM-C as topographic reference data. Given the global availability of ASTER-derived DEMs, the variety of accessible data requires one to validate these products while choosing the most suitable DEM. Many studies address the validation of SRTM and ASTER data by examining global (Rodriguez et al., 2005; Berry et al., 2007; ASTER GDEM Validation Team, 2009) and local approaches (Gorokhovich and Voustianiouk, 2006; Nikolakopoulos et al., 2006). Various factors, such as steep slopes, vegetation, man-made structures, and persistent cloud coverage that causes the number of available images to be low, lead to considerable variation in the quality of these DEMs from one region to another. The best choice among these products requires a thorough assessment of the data and their possible errors with regard to the particular site in which the data will be used. The errors in elevation data generally result from a sum of two components: the horizontal component, which is often referred to as positional accuracy, and the vertical component (i.e., attribute accuracy). However, positional and attribute accuracy usually cannot be separated; the error may be due to an incorrect elevation value at the correct location, a correct elevation value at an incorrect location, or some combination of these two (Nikolakopoulos et al., 2006).

A shift in the DEM may be caused by the limited accuracy of the direct sensor orientation or by differences in the coordinate systems of the cartographic projection applied and the geo-reference of the sensor, which is related to the international terrestrial reference frame (Jacobsen, 2005b). We can assess the elevation attribute accuracy in its nominal position for the models being analyzed through GPS measurements, but assessing the geolocation will be more difficult if the reference DEMs are lacking. To measure this error within a DEM using control point features, the shape of the element to be used as a reference must be recognizable such that its horizontal position can be verified (USGS, 1998). Because finding such a reference element is extremely difficult on coarse-resolution DEMs, different evaluation methods are necessary. Van Niel et al. (2008) found that sub-pixel misregistration between DEMs have a great impact on their altitude differences. Additionally, the researchers observed a strong correlation
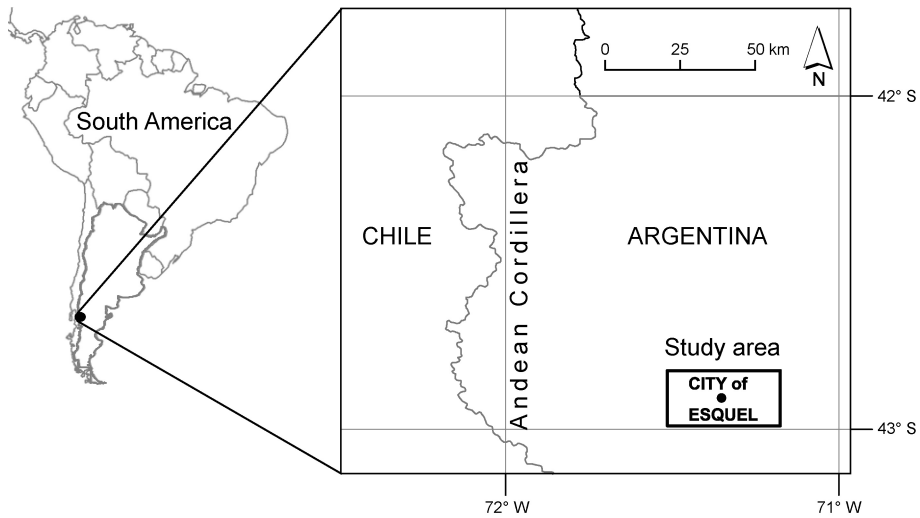
Fig. 1. Study area located on the eastern side of the Patagonian Andes of Argentina.

between the aspect and altitude difference. Therefore, we infer that even small geolocation errors may have a significant influence on the altitude accuracy of the DEMs.

The detection of artifacts and the assessment of morphological details are two major features in this evaluation. Artifacts cause different effects depending on the application of the DEMs, and the defects are frequently propagated to the derived products. With respect to the morphological details, some authors have reported differences between the nominal pixel-size resolution of the DEMs and the actual resolution regarding the information detail provided (Guth, 2006). Visual methods can be important for evaluating those factors and can help counterbalance some of the weaknesses of statistical analysis, as several features and artifacts cannot be discovered with those methods. The analysis of visual quality complements the quality assessment of DEM datasets (Podobnikar, 2009).

The aim of this study is to provide a local evaluation of SRTM-C, the ASTER GDEM, and two DEMs derived from individual ASTER scenes for a site in Patagonia, where no reference precision DEMs are available. We combined geolocation assessment and visual analysis techniques to perform an integrated analysis of the DEMs.

METHODS

Study Area

The study area covers 27 × 20 km around the city of Esquel on the eastern side of the Patagonian Andes and is situated at 42°48′ S to 42°59′ S and 71°31′ W to 71°11′ W (Fig. 1). The area has rugged relief with partial steep slopes and an elevation range of 1710 m (min. 490 m; max. 2200 m). The mean slope is 10.9°, with maximum values around 50°. Approximately 20% of the study area is covered by *Nothofagus sp.* forests and pine plantations. The remaining surfaces include bare soils, steppe grasslands, and meadows.

DEMS

In this study, we assessed an SRTM C-band DEM provided by the CGIAR-CSI (Consultative Group for International Agriculture Research and the Consortium for Spatial Information) and three ASTER DEMs generated via different procedures: ASTER GDEM, a purchased ASTER DEM generated by ERSDAC, and a DEM generated from an individual ASTER scene using the commercial software PCI (Eckert, 2006).

SRTM-C

The original C-band product is missing data in significant areas, due to geometric artifacts, specular reflection of water, phase unwrapping artifacts, and voids due to complex dielectric constants because of the nature of radar remote sensing and the interferometric process applied to create the DEM (Reuter et al., 2007). These data holes are especially concentrated over water bodies and in steep mountainous areas. To correct these phenomena, the CGIAR-CSI used a method based on spatial filtering (Dowding et al., 2004; Jarvis et al., 2004), and compiled the processed SRTM 3 arcsec DEM for the entire globe. The final seamless dataset with filled voids is available on the internet (http://srtm.csi.cgiar.org). The 5° × 5° tile encompassing the study area was downloaded in GeoTiff format with geographic coordinates and datum WGS84. Prior to any analysis, the data were reprojected to the POSGAR 94 Argentinean coordinate system Zone 1 by applying bilinear interpolation resampling with 90 meter spatial resolution output.

ASTER GDEM

The ASTER GDEM is packaged in 1° × 1° tiles in GeoTiff format with geographic coordinates in a 1 arcsec (~30 m) grid. For each tile, two files are delivered: (a) a DEM data file and (b) a quality assessment file, which contains the number of scene-based DEMs contributing to the final DEM value at each pixel and indicates the major data anomalies that have been corrected, including the data source used in the process (ASTER GDEM Validation Team, 2009). The tile corresponding to the study area was downloaded and reprojected to the POSGAR 94 Argentinean coordinate system Zone 1 by applying bilinear interpolation resampling and 30 m output spatial resolution.

ERSDAC-ASTER DEM

In this paper, ERSDAC-ASTER DEM refers to a relative DEM derived from an ASTER image captured on January 13th, 2006. We acquired the product from ERSDAC in Japan, with processing level L4A01 (ERSDAC, 2002), in geographic coordinates with Datum and Ellipsoid WGS84. ERSDAC generated the stereo data with the instrument and spacecraft ephemeris information only for the geolocation. That is, no GPS control points for the individual scene were used. Before analyzing the data, we reprojected them to the POSGAR 94 Argentinean coordinate system Zone 1 by applying bilinear interpolation resampling with 30 meter output spatial resolution.

Table 1. General Characteristics of the Analyzed DEMs

Sensor/source	Elaborated by	Spatial resolution (m)	Elevation reference
SRTM-C	NASA (processed by CGIAR)	90	EGM96 Geoid
ERSDAC-ASTER DEM	ERSDAC	30	WGS84 Ellipsoid
ASTER GDEM	METI-NASA	30	EGM96 Geoid
ASTER DEM	Eckert (2006)	30	Intl. 1924 Ellipsoid

ASTER DEM

ASTER DEM describes an absolute DEM generated by Eckert (2006) with ASTER image data that were captured on January 18, 2002. Eckert generated the DEM with the PCI Geomatics 8.0 Ortho Engine with 41 ground control points (GCPs) (x, y, z) measured with GPS differential correction techniques, and extracted the DEM with 30 m spatial resolution and mean RMS errors of the bundle adjustment of 13.35 m in x and 14.25m in y. The projection system used in the generation of this DEM was the former national Argentinian system Gauss-Krüger, Zone 1, with local Datum Campo Inchauspe and Ellipsoid International 1924 (Eckert, 2006).

The assessed DEMs are related to different vertical geodetic reference systems (Table 1). To compare the datasets, we converted all of the altitude values in meters above the WGS84 ellipsoid.

Geolocation Assessment

Because any elevation error could be caused by an x, y displacement of the DEM instead of an altitude difference, the geolocation assessment complements the altitude evaluation of the data. This feature is critical for relative DEMs, which were generated without any ground control points and, therefore, lack precise geo-referencing. Typically, the methods applied for this assessment are based on high-precision reference DEMs (Sun et al., 2003; Nikolakopoulos et al., 2006). However, this type of data is not always available. We performed the geolocation analysis for SRTM-C and the two ASTER DEMs generated without GCPs. We applied a GPS track method, which allows us to determine the horizontal position in which the shape of the DEM best fits a precisely localized track (Rodriguez et al., 2005). Nine GPS tracks along roads at different altitudes were measured throughout the study area, with regular horizontal distances using a Trimble GeoXT in a carrier-phase mode. We performed a post-processing differential correction of the GPS data with measurements from a Trimble 4600 L base. In this way, we were able to achieve a precision level of 0.7 m. In total, 22 sample track segments containing 40 points distributed across 2000 meters of length were selected and shifted over a 5 m–spaced square grid composed of 30 positions in the north-south and east-west directions from the original (nominal position). For each new position, we calculated the height differences between the GPS points and the DEM and determined the standard deviations of the differences. By doing so, we

accounted for a total of 880 points in 3600 different positions. The position with the smallest standard deviation of the differences was considered the best fit of the DEM to the real landform (optimal position). We calculated the geolocation error as the difference between the x, y nominal and optimal positions for each of the 22 segments. We statistically analyzed the geolocation errors and determined the x, y mean geolocation error, the standard deviation of the x, y geolocation error, and the x, y linear root mean square error (RMSE) (ACIC, 1968). We calculated the circular error of 90% of the data by following FGDC (1998). A Shapiro Wilk's test was performed to test the normality of the x, y errors. To assess the bias in the x, y geolocation errors, we checked against a mean error equaling 0 hypothesis with a *t*-test.

Elevation Assessment

The reference data for the elevation assessment consisted of ground control points measured with differential GPS. Given a certain dependence of the DEM error distribution on slope, aspect, and land cover (Eckert et al., 2005), the assessment area was located in zones of bare soils and steppe grasslands. The set of road segments with 43 km in total length chosen for this purpose had a representative variability of slopes, altitude, and terrain roughness. Of the 1660 resulting measurements, we sampled 78 randomly chosen points for the analysis. We used equation 1 (Steel et al., 1997) to approximate the needed sample size:

$$n \geq \left(\frac{2z_{1-\alpha/2}\sigma}{c} \right)^2 \tag{1}$$

where σ denotes the population's standard deviation and *c* indicates the amplitude required for the confidence interval (CI) with a confidence of $(1-\alpha)$% in the estimated population mean value. In accordance with the average values reported by Berry et al. (2007) and Rodriguez et al. (2005) in their papers addressing SRTM-C data in South America and on a global level, we adopted a maximum expected variance of 100 m and a confidence interval amplitude of 5 m with $\alpha = 0.5$. Doing so led to a required minimum sample size of 61 points. Based on this minimum size, we randomly selected 78 points from the original 1166. We tested the reliability of the RSME estimation based on the selected points with a non-parametric model named UAL, which was specifically developed to evaluate DEMs (Aguilar et al., 2007).

In accordance with precision requirements suggested by Maune (2007), the reference points were distributed between 521 and 1519 m elevation, with a mean precision of 0.35 m in the horizontal direction and 0.24 m in the vertical direction. At the geographic coordinate of every sampled point, we extracted the elevation values from the DEMs and defined the difference between the measured and the extracted height value as an error. We statistically analyzed the elevation differences between the DEMs and the control points and determined the mean error, standard deviation, and root mean square error (RMSE) to assess the elevation accuracy of the DEMs. If the elevation errors were not normally distributed, we applied non-parametric descriptive statistics, as proposed by Höhle and Höhle (2009). We evaluated the statistical significance of the error bias by employing a *t*-test against the hypothesis of mean values equaling 0.

For those DEMs that showed a horizontal bias in the geolocation assessment, we performed further analysis. We moved each DEM toward the position that eliminated the bias and applied the elevation assessment afterwards.

To compare the behavior of the whole DEMs with and without shifting to the best-fit geolocation position, we compared the SRTM-C and ERSDAC ASTER DEMs with each other and against the GDEM. We performed two raster subtractions for each DEM pair: one with the raster at its nominal position and the other with each DEM moved toward the magnitude and direction that eliminated their geolocation bias.

At 45 of the 78 control points, the slope was measured with a clinometer and classified into two slope classes (>10º and <10º) in accordance with Gorokhovich and Voustianiouk (2006). We compared the absolute height error of each class by utilizing an independent measures t-test. At the points with >10º slopes, the aspect was determined with a compass and classified into one of four classes (NE, SE, NW, and SW). Then we performed the same statistical analysis that we conducted for the slope classes.

Visual Quality Analysis

We performed visual analysis on the DEM-derived products. We generated contour lines with a 50 m interval and shaded relief with ERDAS 9.1 software. For a systematic analysis, we divided the study area into 140 cells of 400 ha and observed in each of them the following categorical variables:

Based on shaded relief:

> • terrain roughness (high–moderate–low)

Based on shaded relief and contour lines:

> • artifact frequency (high–moderate–low)

> • definition (high–moderate–low)

We conducted a correspondence analysis of these variables with the software InfoStat (www.infostat.com.ar). This technique graphically displays the multivariate categorical data by deriving coordinates to represent the categories of both the row and column variables, which may then be plotted to graphically represent the association patterns among the variables.

RESULTS

Geolocation Assessment

The statistical results of the geolocation analysis are presented in Table 2. Because the samples were moved on to a grid with a centered origin, the negative values in x and y indicate a geolocation error in the western and southern directions, respectively.

The x, y error distribution for the 22 analyzed segments is shown in Figure 2, where biases of the location errors are in the opposite directions for the SRTM-C and ERSDAC-ASTER DEMs. In contrast, we found no tendency of the geolocation errors for GDEM, which certainly show a higher dispersion in magnitude and direction.

Table 2. Geolocation Error Assessment Statistics for the Analyzed DEMs

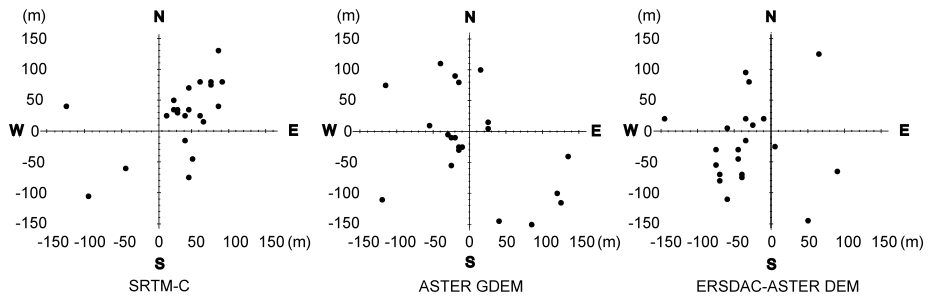| Statistics (m)	DEMs		
	SRTM-C	ASTER GDEM	ERSDAC-ASTER DEM
Mean error x	28.4	2.3	−32.7
Mean error y	25.9	−16.6	−20.7
Standard deviation x	53.4	67.1	50.9
Standard deviation y	56.4	76.9	65.5
Linear mean error	77.3	84.3	83.6
Linear RMSE	85.0	101.1	89.8
Circular error (90%)[a]	129.1	153.4	136.2

[a]Calculated as proposed by FGDC (1998).

Fig. 2. Geolocation error distribution for the 22 analyzed segments in the SRTM-C, ASTER GDEM, and ERSDAC-ASTER DEM. Each point corresponds to the difference between the nominal and optimal positions from each segment.

Elevation Assessment

The elevation errors determined by the comparison of the 78 GPS control points with the corresponding elevation values of the four DEMs are presented in Table 3. In all of the cases except SRTM-C, the elevation errors were normally distributed. The SRTM-C showed a median error close to 0, with a narrow distribution of the error values containing 68.3% of the data, as illustrated in Figure 3. Although this dataset presented many extreme errors that lead to the highest error range, it had the lowest RMSE value, followed by the ASTER GDEM. For the ERSDAC-ASTER DEM and ASTER GDEM, we detected a significant negative bias (*t*-test, null hypothesis: mean error = 0), with −8.1 and −6.0 m, respectively. These findings indicate that both datasets underestimate height values (Table 3). The GDEM errors showed the lowest range and also the lowest standard deviation (*f*-test GDEM vs. ERSDAC-ASTER DEM, $p = 0.035$).

The height evaluations of SRTM-C and ERSDAC-ASTER after they were moved to their optimal positions showed a decreased RMSE for both DEMs. This result is

Table 3. Height Error Statistics for the Analyzed DEMs

Statistics (m)	DEMs					
	SRTM-C	ASTER GDEM	ERSDAC ASTER DEM	ASTER DEM	SRTM-C (post-shift)	ERSDAC ASTER DEM (post-shift)
Mean error	–0.6	–6.0	–8.1	2.1	0.4	–8.4
Median error	–0.1	–4.4	–7.5	4.0	0.7	–8.5
Standard deviation	8.3	7.3	9.3	10.4	7.2	7.3
RMSE	8.3 ± 2.9[c]	9.4 ± 2.3[c]	12.3 ± 2.8[c]	10.5 ± 1.9[c]	7.2	11.1
Min. error	–37.7	–28.5	–37.6	–28.5	–37.6	–27.6
Max. error	24.7	7.9	15.2	26.3	22.5	14.6
Error range	62.4	36.4	52.8	54.8	60.1	42.2
SW-W (p < 0.01)[a]	**	n.s.	n.s.	n.s.	**	n.s.
t-test again 0 (p < 0.001)[b]		***	***			***

[a]** = error data not normal (Shapiro Wilk's test with $p < 0.01$); n.s. = error data normal (Shapiro Wilk's test $p > 0.01$).
[b]*** = mean error significantly different from 0 (t-test $p < 0.01$).
[c] Confidence interval with significance of 95% calculated from Aguilar et al. (2007).

probably caused by the decreasing standard deviation (random error), whereas the mean values (tendency) retained their signs and magnitudes (Table 3).

The height differences between the DEMS showed the mean values according to the tendencies detected in the analysis using the GPS control points (Table 4). These mean values persisted in the difference calculated between SRTM-C and ERSDAC-ASTER DEMs after these DEMs were moved to their optimal positions. However, their distributions were more compact afterwards and, consequently, had lower standard deviations and RMSE (Figure 4 and Table 4).

The height accuracy of all DEMs diminished in the situations in which the measured slope exceeded 10°. We used an independent measures t-test to assess this situation and found that the absolute errors in the elevations were significantly higher for the terrains with slopes exceeding 10° compared with the areas in which the slopes were less than 10° in the case of ERSDAC-ASTER DEM ($p = 0.01$), SRTM-C ($p = 0.01$), and ASTER DEM ($p = 0.01$). No significant differences were found for ASTER GDEM. The average error magnitude was almost three times higher in SRTM-C and two times higher in ERSDAC-ASTER DEM and ASTER DEM for the slopes exceeding 10° than for the slopes less than 10°.

In the ERSDAC-ASTER DEM, we found significant differences (independent measures t-test) in the absolute elevation errors among the following aspects: NE vs. SE ($p = 0.0038$); NE vs. SW ($p = 0.0019$); and NW vs. SW ($p = 0.049$). The other DEMs showed non-significant differences in all cases. Although for SRTM-C, the NE and SW exposed sites had mean absolute errors twice as high as the SE and NW
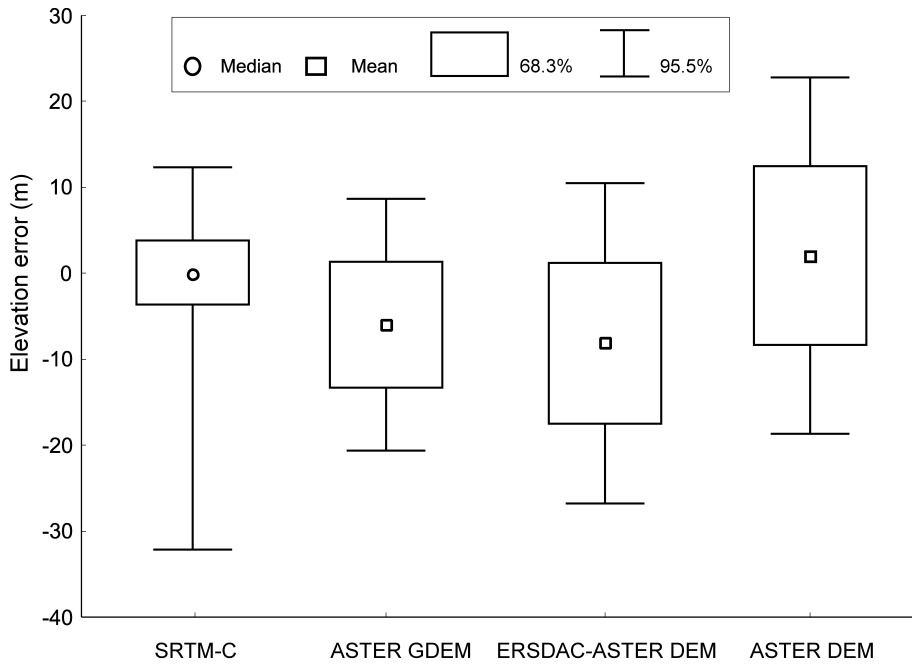
Fig. 3. The elevation error dispersion of the DEMs for the 78 analyzed DGPS points.
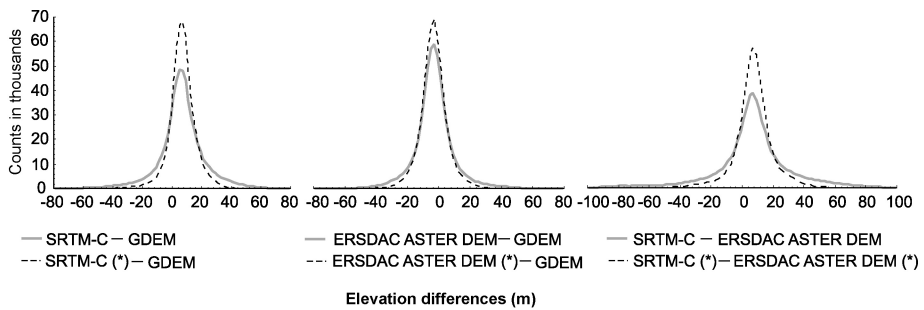

Fig. 4. Histograms with the elevation differences among the DEMs, which are obtained from the subtraction of the rasters in their nominal and calculated optimal positions. Asterisk symbols (*) correspond to DEMs that shifted to their mean optimal positions.

exposed sites, this difference could not be statistically analyzed because normality was not accomplished (Table 5).

Visual Quality Analysis

The visual analysis revealed differences between the DEMS that are difficult to describe with statistical techniques. The shaded relief images showed major arti-facts similar to those in Figures 5A and 5B, where the mountain peak appears to be

Table 4. Statistics for the Elevation Differences Between the DEMs Obtained from the Subtraction of Rasters in Their Nominal and Calculated Mean Optimal Positions[a]

DEMs subtracted	Statistics (m)				
	Mean	Stand. Dev.	RMSE	Max.	Min.
{SRTM-C} – {ASTER GDEM}	7.0	16.0	17.2	97	−116
{SRTM-C (shf)} – {ASTER GDEM}	7.3	9.4	11.8	62	−80
{ERSDAC-ASTER } – {ASTER GDEM}	−2.8	13.2	13.2	107	−164
{ERSDAC-ASTER (shf)} – {ASTER GDEM}	−3.0	9.6	9.8	120	−155
{SRTM-C} – {ERSDAC-ASTER}	9.6	24.8	26.4	168	−118
{SRTM-C (shf)} – {ERSDAC-ASTER (shf)}	10.1	12.5	16.0	149	−98

[a] (shf) corresponds to DEMs that shifted to their optimal positions.

Table 5. Height Error Values of Different Slope and Aspect Classes for the Analyzed DEMs[a]

		SRTM-C	ASTER GDEM	ERSDAC-ASTER DEM	ASTER DEM
Slope <10º		4.6 ± 1.0	7.3 ± 1.4	8.5 ± 1.3	5.8 ± 1.1
Slope >10º		12.7 ± 2.5	10.1 ± 1.6	15.4 ± 1.7	11.9 ± 1.7
Aspect	NE	25.7 ± 5.3	8.7 ± 1.7	18.3 ± 3.7	6.9 ± 1.9
	SE	10.4 ± 3.5	14.3 ± 3.4	13.8 ± 2.1	19.3 ± 3.6
	SW	25.8 ± 6.7	9.0 ± 2.1	7.3 ± 4.1	11.3 ± 3.5
	NW	10.2 ± 2.9	8.8 ± 2.2	16.1 ± 2.4	10.2 ± 2.1

[a] Errors are expressed as absolute height error ± the standard error of the mean.

a depression and a flat area in the ERSDAC-ASTER DEM and the ASTER DEM, respectively. Each of the three ASTER-derived DEMs showed artifacts in the systematic visual analysis. These artifacts were mainly small negative or positive anomalies similar to the ones shown in Figure 5A. We found artifacts similar to those shown in Figures 5C and 5D in the contour lines derived from all of the DEMs.

The multivariate analysis showed a strong correspondence between the ERSDAC-ASTER DEM and the high-level definition and between the SRTM-C and the low-level definition. The ERSDAC-ASTER DEM exhibited a high correspondence with medium and high artifact frequency levels. In contrast, high artifact frequency was in all of the DEMs related to smooth terrain (Fig. 6).
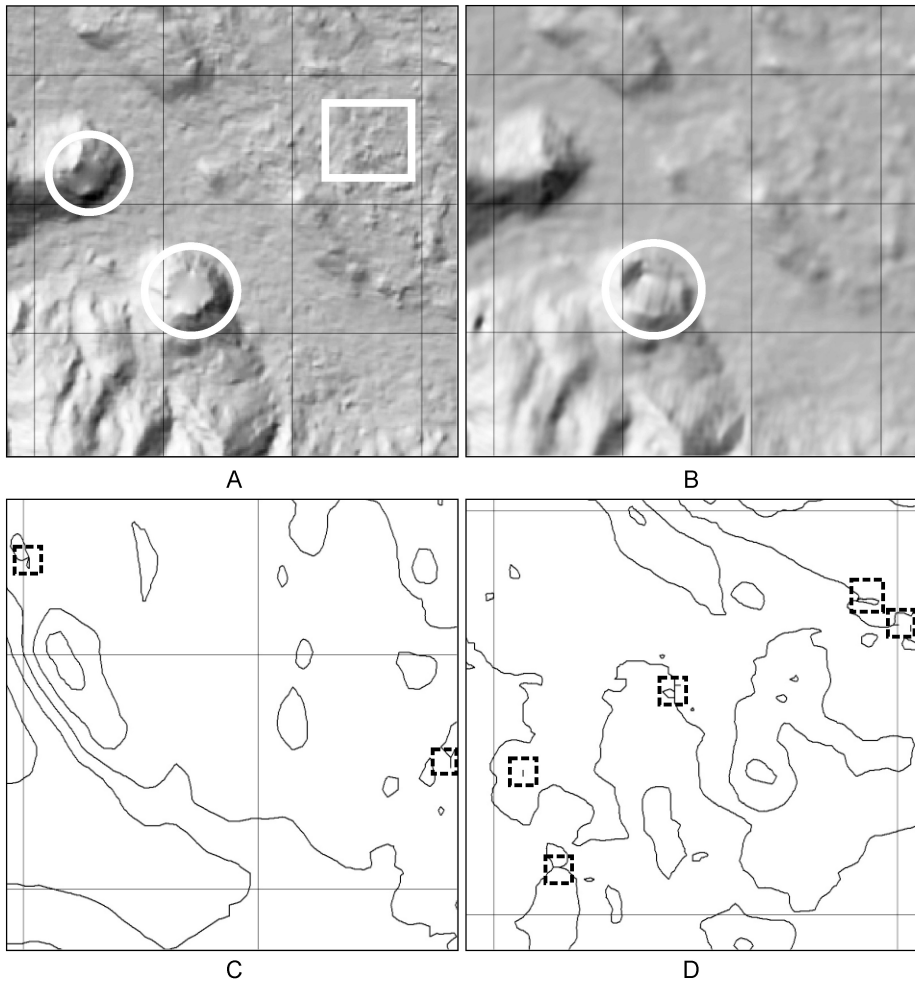
Fig. 5. DEM-derived products used for the visual analysis. A and B. Shaded relief images derived by the (A) ERSDAC-ASTER DEM and (B) ASTER DEM. White circles indicate the major artifacts, and white rectangles indicate the minor artifacts that correspond to the small negative and positive anomalies. C and D. Contour lines using 50 m equidistance derived by the (C) SRTM-C and (D) ERSDAC-ASTER DEM. The squares with dotted lines are examples of the anomalies considered to be artifacts. Each square of the grid corresponds to an area of 400 ha.

DISCUSSION

In the absence of a reference DEM for the study area, the geolocation assessment method performed in this study allowed us to determine the magnitude and direction of the horizontal location errors in the three analyzed DEMs. The use of 22 track segments allowed us to detect a systematic component (bias) in the geolocation errors of the SRTM-C and ERSDAC-ASTER DEMs. This result was confirmed by a reduction in the RMS elevation error after the bias was eliminated.
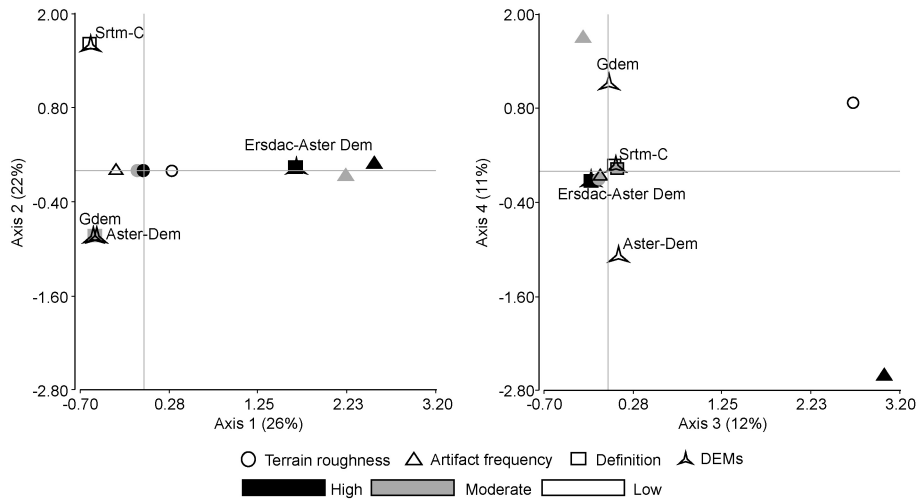
Fig. 6. Correspondence analysis for the categorical variables from the visual analysis.

Even after the DEMs with geolocation bias (i.e., SRTM-C and ERSDAC-ASTER) were shifted to their optimal positions, the mean height errors remained unmodified. Additionally, in the comparison after the raster subtractions, the mean differences between the DEMs in the original and those in the moved positions did not show significant changes. Nevertheless, the dispersions of the height errors and of the differences between the DEMs decreased after the DEMs shifted to their optimal positions. This finding may indicate that the mean height error value is not affected by systematic localization errors, at least not if it has the magnitude observed in the present study. However, the systematic localization errors affect the dispersion of the height error distribution, as shown in Tables 3 and 4. This finding is in accordance with the results reported by Van Niel et al. (2008), who conducted an analysis through induced misregistration. These authors found that even a localization difference on the sub-pixel level may cause elevation differences between DEMs of the same or higher magnitudes as their actual elevation differences. The magnitude of the elevation differences caused by misregistration further increases in areas with steep slopes.

Van Niel et al. (2008) also observed that misregistration is the source of a strong correlation between the DEMs' elevation differences and aspects, which can be modeled by a sinusoidal wave. In the case of a systematic misregistration, the highest differences are associated with the aspects in its direction and the opposite one. The opposite aspects will show mean difference values similar to the general mean difference values, but one will be greater and the other will be less than the general mean difference value. If we apply these findings to a DEM height error caused by a systematic localization error, these conclusions allow us to infer that the absolute elevation error reaches its maximum on the aspect equal to the direction of the location error and its opposite. We can observe this result in the ERSDAC-ASTER and SRTM-C DEMs (Table 5). The elevation differences induced by the location errors were compensated for in the opposite aspects. This finding explains why the mean difference values did

not change significantly between the original and the shifted DEMs, but the dispersions of their distributions did.

Using a reference DEM in four areas in the United States, Hofton et al. (2006) found systematic geolocation errors between 15 and 25 meters in the NW direction in the 1 arc second resolution SRTM-C DEM. These values are similar to the bias of 28.4 m in x and 25.9 m in y that was found in our study area. Rodriguez et al. (2005) also reported a bias in the same direction as that found in our study for all of South America after evaluating the SRTM-C DEM at the global level. The results of the geolocation assessment for the ERSDAC-ASTER DEM correspond to the nature of the DEM generated without GCPs. The observed horizontal geolocation accuracy was consistent with the spacecraft position accuracy of 50 m (3 standard deviations) reported by ERSDAC. Toutin (2008) recommends georeferencing this type of DEM to a map coordinate system with GCPs because of inadequate pointing and ephemeris information (errors about 300 m in x, y). These extreme values are higher than those found in the analyzed ERSDAC-ASTER DEM scene, but closer to the highest error values found for the ASTER GDEM (135 in x and –150 in y). Jacobsen and Passini (2010) reported geolocation shift values of –2.9 to 7.8 m in x and –8.7 to 11.6 m in y for three tiles in North America, one in Jordan, and one in France for the GDEM. These values are similar to the values reported by the ASTER GDEM Validation Team (2009) for the Global Validation Analysis. Because the dispersion of geolocation error values has not been reported in any of the studies, the high values found for the GDEM in this work may not be comparable. The varying number of scenes used to generate the DEM in different sectors of the present tiles may have caused the high dispersion given that a specific geolocation error component for each scene depends on the spacecraft position accuracy. In the regions in which the acquisition of optical imagery is difficult because of persistent cloudiness, the variability of the number of used scenes is even higher, and one must expect significant differences in accuracy for the regions with distinct cloud cover regimes.

Apart from their influence on the elevation error, other consequences of the DEM location errors have been described. Some processes, such as radiometric corrections of satellite imagery to remove topographic effects, are likely to be affected by the location errors of the used DEMs. According to Richter (1998), in cases of critical geometries, half a pixel offset between the imagery and the DEM may lead to large relative reflectance errors that exceed 100%. Imagery orthorectification accuracy is also related to the geolocations of the DEMs used (Toutin, 1995). The method described in this study allows one to detect and correct systematic geolocation errors, though non-systematic errors are difficult to correct. Nevertheless, the DEMs' co-registration processes were successfully performed in other regions in which accurate reference DEMs are available (Jacobsen, 2005a; Karkee et al., 2008). The difficulties in identifying structures or objects from reality in coarse-resolution DEMs prevent us from correcting the location errors with data such as GCPs in the areas without available reference products.

We found that the elevation errors observed for SRTM-C in the present study are in the same range as those documented in past studies in various parts of the world (Rodriguez et al., 2005; Gorokhovich and Voustianiouk, 2006). We find that random error is the major component in the data in which we observed unbiased height errors. However, we must consider that the GCPs were only measured in non-forest areas

to avoid errors caused by forest canopy heights. The strong influence of outliers was probably due to steep slopes at the sample points, whereas our dataset had mainly medium and flat slopes.

The height error bias for the ASTER relative DEM products L4A01 depends partly on the spacecraft position accuracy. ERSDAC (2002) reports height error biases ranging from –8 to 5 m for five sites in Japan. The bias observed in the present study is located well within this range (Table 3). The GDEM height error bias also exhibited variable magnitudes and signs in the tiles assessed by the ASTER GDEM Validation Team (2009). Using a reference DEM for comparison purposes, Pagnutti and Ryan (2009) found biases of –8.6, –10.4, and –2.5 m for the GDEM in Alaska, Russia, and India, respectively. Although these biases are close to those found in this study, the RMSE values of 15.4, 13.1, and 11.7 m reported for these three sites are slightly higher as a result of the higher error variability. The ASTER GDEM Validation Team (2009) reported that the level of the height error values in the GDEM depends on the number of tiles used in the DEM generation process, with a significant improvement in the RMSE values in the areas in which more than four tiles are used in the product generation process. The decrease in the error's standard deviation in the areas with high numbers of scenes used for DEM generation in the GDEM would explain this improvement in the RMSE (ASTER GDEM Validation Team, 2009). The major part of the study area in this work has more than eight tiles, and its better performance with regard to the other two ASTER DEMs is shown by the weaker random component of the elevation error.

The "absolute DEM" condition of the ASTER DEM was reflected in its lower elevation bias with respect to the two other ASTER-derived DEMs. Its higher RMSE (10.5 m) can be explained by the greater influence of the random error (standard deviation 10.4 m), which suggests low precision levels in the matching performance. The metadata for this imagery report low gain values for the VNIR bands, which has been mentioned as one of the causes of a decrease in the precision of this process (Hashimoto, 1997; Lencinas, 2009). The number of GCPs utilized to generate this DEM was higher than those reported by other authors (Hirano et al., 2003; Marangoz et al., 2005). According to these researchers, the limit at which an increment in the number of points does not translate into an increase in accuracy is far below the number of points utilized by Eckert (2006). The ERSDAC-ASTER DEM is a raw product in which no error elimination filters are applied and VNIR low gains are used in its production. The high frequency of artifacts found in the visual analysis confirms this finding. However, this DEM had the highest definition. After generating the ASTER DEM, Eckert (2006) partially removes the artifacts by applying smoothing filters, which causes a loss of definition that leads to a medium-level definition. GDEM also presents a medium definition level, but the use of various ASTER scenes in its generation procedure may lead to a decrease in the artifact frequency and the error magnitude. However, an undesired consequence of the GDEM generation process was the presence of additional artifacts corresponding to the borders of the DEM areas with different number of scenes used in their generation. These additional artifacts cause the quality of the GDEM to diminish (ASTER GDEM Validation Team, 2009).

The nominal resolution of the DEMs may not coincide with the actual information that they contain. According to Jacobsen and Passini (2010), the morphological detail of the ASTER GDEM is in the range corresponding to 60 m point spacing. Conversely,

according to the ASTER GDEM Validation Team (2009), the real resolution of the GDEM is not much finer than 120 m. In the case of the SRTM-C, the 1 arc second version for some authors is closer to 60 or 90 m (Crippen, 2005; Hensley, 2005), and the SRTM-C's 3 arc second products obtain a real resolution close to the nominal one (Guth, 2006). This study did not assess the absolute resolution of the analyzed DEMs, but the visual analysis indicates that in our study area, the three ASTER models provide a greater amount of information than those obtained with the SRTM-C. This higher information level still exists even in the contour lines generated from the ASTER models resampled to 90 m.

CONCLUSIONS

We found geolocation errors for all three analyzed DEMs at levels that may affect their performance, depending on their applications. The linear RMSE was 85.0 m for the SRTM-C, 89.8 m for the ERSDAC-ASTER DEM, and 101.1 m for the ASTER GDEM. The systematic geolocation errors found in the SRTM-C and ERSDAC-ASTER DEMs do not seem to affect their elevation bias but determine an increase in the random height error that would be greater in those aspects corresponding to the direction of that systematic geolocation error. The GDEM exhibited a high variability in the geolocation error, which could be associated with a lower geometrical coherence because of its production procedure. Future researchers should conduct tests with high-precision, accurate datasets to determine whether registering with these datasets improves the performance of GDEMs. The results obtained in the geolocation assessment indicate the need for local evaluations of localization errors if global DEMs are used, especially for applications that could be significantly affected by these errors.

SRTM-C exhibited a narrow elevation error distribution but with a wide range, which is probably associated with a higher sensitivity to steep slopes. The ASTER GDEM showed a lower elevation error dispersion compared with the other two ASTER DEMs.

SRTM-C displayed a higher data homogeneity, which translates into higher reliability because it is a dataset with accurate error-correction processes. In contrast, various studies have found that the GDEM exhibits a high variability of noise depending on the study area and, therefore, the number of scenes used for the DEM generation process. It would be useful if researchers could form a global GDEM error correction process given its apparently higher morphological resolution. This feature is considered if more detailed information is required.

REFERENCES

ACIC (Aeronautical Chart and Information Center, 1968, *Principles of Error Theory and Cartographic Applications*, St. Louis, MO: ACIC Technical Report No. 96, U.S. Air Force.

Aguilar, F. J., Aguera, F. and M. A. Aguilar, 2007, "A Theoretical Approach to Modeling the Accuracy Assessment of Digital Elevation Models," *Photogrammetric Engineering & Remote Sensing*, 73(12):1367–1379.

ASTER GDEM Validation Team:METI/ERSDAC, NASA/LPDAAC, USGS/EROS, 2009, "ASTER Global DEM Validation Summary Report" [http://www.ersdac .or.jp/GDEM/E/image/ASTERGDEM_ValidationSummaryReport_Ver1.pdf].

Becek, K., 2008, "Investigation of Elevation Bias of the SRTM C- and X-Band Digital Elevation Models," in *Proceedings of the XXI Congress of ISPRS,* Beijing, China, XXXVII(B1-1):105–110.

Berry, P. A. M., Garlick, J. D., and R. G. Smith, 2007, "Near-Global Validation of the SRTM DEM Using Satellite Radar Altimetry," *Remote Sensing of Environment*, 106(1):2869–2874.

Blanchard, S. D., Rogan, J., and D. W. Woodcock, 2010, "Geomorphic Change Analysis Using ASTER and SRTM Digital Elevation Models in Central Massachusetts, USA," *GIScience & Remote Sensing*, 47(1):1–24.

Crippen, R., 2005, "Topographic Change and Topographic Data Evaluation: SRTM Compared to NED across the Entire USA," in *Proceedings of The Shuttle Radar Topography Mission—Data Validation and Applications Workshop*, Reston, Virginia, June 14–16.

Di, B. E., Chen, N. S., Cui, P., Li, Z. L., He, Y. P., and Y. C. Gao, 2008, "GIS-Based Risk Analysis of Debris Flow: An Application in Sichuan, Southwest China," *International Journal of Sediment Research*, 23(2):138–148.

Dowding, S., Kuuskivi, T, and X. Li, 2004, "Void Fill of SRTM Elevation Data— Principles, Processes, and Performance," in *Proceedings of the ASPRS 2004 Fall Conference, Images to Decisions: Remote Sensing Foundations for GIS Applications*, Kansas City, Missouri, September 12–16 (CD-ROM).

Eckert, S., 2006, *A Contribution to Sustainable Management in Patagonia: Object-Oriented Classification and Forest Parameter Extraction Based on ASTER and Landsat ETM+ Data*, Zurich, Switzerland: Universität Zürich, 191 p.

Eckert, S., Kellenberger, T., and K. Itten, 2005, "Accuracy Assessment of Automatically Derived Digital Elevation Models from ASTER Data in Mountainous Terrain," *International Journal of Remote Sensing*, 26:1943–1957.

Elaksher, A. F., 2009, "Using LIDAR-Based DEM to Orthorectify Ikonos Panchromatic Images," *Optics and Lasers in Engineering*, 47(6):629–635.

ERSDAC (Earth Remote Sensing Data Analysis Center), 2002, *ASTER User's Guide Part III. DEM Product (L4A01)*, 19 p.

Fahsi, A., Tsegaye, T., Tadesse, W., and T. Coleman, 1999, "Incorporation of Digital Elevation Models with Landsat-TM Data to Improve Land Cover Classification Accuracy," *Forest Ecology and Management*, 128:57–64.

FGDC (Federal Geographic Data Committee), 1998, *Geospatial Positioning Accuracy Standards. Part 3: National Standard for Spatial Data Accuracy*, Washington, DC: FGDC, FGDC-STD-007.3-1998.

Finney, M. A., 1998, *FARSITE: Fire Area Simulator—Model Development and Evaluation*, Ogden, UT: U.S. Department of Agriculture, Forest Service, Rocky Mountain Research Station, Research Paper RMRS-RP-4, 47 p.

Gonçalves, J. A. and A. M. Oliveira, 2004, "Accuracy Analysis of DEM-Derived from ASTER Imagery," *International Archives of Photogrammetry and Remote Sensing*, 35:168–172.

Gorokhovich, Y. and A. Voustianiouk, 2006, "Accuracy Assessment of the Processed SRTM-Based Elevation Data by CGIAR Using Field Data from USA and Thailand

and Its Relation to the Terrain Characteristics," *Remote Sensing of Environment,* 104:409–415.

Guth, P. L., 2006, "Geomorphometry from SRTM : Comparison to NED," *Photogrammetric Engineering & Remote Sensing*, 72(3):269–277.

Hashimoto, T., 1997, "DEM Generation from AVNIR Stereo Images," *Geocarto International*, 12(4):35–37.

Hensley, S., 2005, "From Raw Data to Digital Elevation Map," in *Proceedings of The Shuttle Radar Topography Mission—Data Validation and Applications Workshop*, June 14–16, Reston, Virginia.

Hirano, A., Welch, R., and H. Lang, 2003, "Mapping from ASTER Stereo Image Data: DEM Validation and Accuracy Assessment," *ISPRS Journal of Photogrammetry & Remote Sensing*, 57:356–370.

Hofton, M., Dubayah, R., Blair, J. B., and D. Rabine, 2006, "Validation of SRTM Elevations over Vegetated and Non-vegetated Terrain Using Medium Footprint Lidar," *Photogrammetric Engineering & Remote Sensing*, 72(3):279–285.

Höhle, J. and M. Höhle, 2009, "Accuracy Assessment of Digital Elevation Models by Means of Robust Statistical Methods," *ISPRS Journal of Photogrammetry and Remote Sensing*, 64:398–406.

Jacobsen, K., 2001, "New Developments in Digital Elevation Modelling," *Geoinformatics*, 6:18–21.

Jacobsen, K., 2005a, "Analysis of SRTM Elevation Models," *EARSEL 3D- RS Workshop*, Porto 2005 [http://www.ipi.uni-hannover.de].

Jacobsen, K., 2005b, "DEMs Based on Space Images versus SRTM Height Models," in *Proceedings of the ASPRS 2005 Annual Conference*, Baltimore, Maryland, USA, March 7–11 (CD-ROM).

Jacobsen, K. and R. Passini, 2010, "Analysis of ASTER GDEM Elevation Models," in *Proceedings of the ISPRS Commission I Mid-Term Symposium "Image Data Acquisition—Sensors & Platforms*," Calgary, Canada, June 15–18, Vol. XXX–VIII, Part 1 (CD-ROM).

Jarvis, A., Rubiano, J., Nelson, A., Farrow, A., and M. Mulligan, 2004, *Practical Use of SRTM Data in the Tropics: Comparisons with Digital Elevation Models Generated from Cartographic Data*, Cali, Colombia: Centro Internacional de Agricultura Tropical (CIAT) Working Document, Vol. 198, 32 pp.

Karkee, M., Steward, B. L., and S. A. Aziz, 2008, "Improving Quality of Public Domain Digital Elevation Models through Data Fusion," *Biosystems Engineering*, 101:293–305.

Kenward, T., Lettenmaier, D. P., Wood, E. F., and E. Fielding, 2000, "Effects of Digital Elevation Model Accuracy on Hydrologic Predictions," *Remote Sensing of Environment,* 74(3):432–444.

Lencinas, J., 2009, "Bosques de Montaña y Teledetección Óptica Espacial: Desarrollo y Perspectivas (Mountain Forests and Remote Sensing Space Optics: Development and Prospects," In *Proceedings of the XIII° Congreso Forestal Mundial*, Buenos Aires, Argentina, October 18–23. *Tema: 1. Bosques y biodiversidad. Subtema: 1.1. Situación de los bosques y técnicas para su evaluación* (*Theme 1. Forests and Biodiversity. Sub-theme 1.1. State Forests and Assessment Techniques*) , 13 pp. (CD-ROM).

Mahmood, S. A. and R. Gloaguen, 2011, "Analyzing Spatial Autocorrelation for the Hypsometric Integral to Discriminate Neotectonics and Lithologies Using DEMs and GIS," *GIScience & Remote Sensing*, 48(4):541–565.

Marangoz, A., Büyüksalih, G., Büyüksalih, I., and U. Sefercik, 2005, "Geometric Evaluation, Generation from Along-Track Stereo ASTER Automated DEM and Orthoimage Images," In *Proceedings of 2nd International Conference on Recent Advances in Space Technologies, RAST 2005, IEEE*, 505–510.

Maune, D. F. (Ed.), 2007, *Definitions in Digital Elevation Model Technologies and Applications: The DEM Users Manual*, 2nd edition, Bethesda, MD: American Society for Photogrammetry and Remote Sensing, 551 p.

Nelson, A., Reuter, H. I., and P. Gessler, 2009, "DEM Production Methods and Sources," in *Developments in Soil Science*, Hartemink, A. E and A. B. McBratney (Eds.), Amsterdam, The Netherlands: Elsevier, 65–85.

Nikolakopoulos, K., E. Kamaratakis, and N. Chrysoulakis, 2006, "SRTM vs. ASTER Elevation Products. Comparison for Two Regions in Crete, Greece," *International Journal of Remote Sensing*, 27(21):4819–4838.

Pagnutti, M. and R. E. Ryan, 2009, "Automated DEM Validation Using ICESAT GLASS DATA," in *Proceedings of the ASPRS/MAPPS Fall Conference*, San Antonio, Texas, November 16–19 [http://www.asprs.org/publications/proceedings/sanantonio09].

Pike, R., 2000, "Geomorphometry: Diversity in Quantitative Surface Analysis," *Progress in Physical Geography*, 24:1–20.

Podobnikar, T., 2009, "Methods for Visual Quality Assessment of a Digital Terrain Model," *Sapiens*, 2(2):1–10.

Qi, S., Brown, D. G., Tian, Q., Jiang, L., Zhao, T., and K. M. Bergen, 2009, "Inundation Extent and Flood Frequency Mapping Using LANDSAT Imagery and Digital Elevation Models," *GIScience & Remote Sensing*, 46(1):101–127.

Reuter, H. I., Nelson, A., and A. Jarvis, 2007, "An Evaluation of Void-Filling Interpolation Methods for SRTM data," *International Journal of Geographical Information Science*, 21(9):983–1008.

Riaño, D., Chuvieco, E., Salas, J., and I. Aguado, 2003, "Assessment of Different Topographic Corrections in Landsat-TM Data for Mapping Vegetation Types," *IEEE Transactions on Geoscience and Remote Sensing*, 41(5):1056–1061.

Richter, R., 1998, "Correction of Satellite Imagery over Mountainous Terrain," *Applied Optics*, 37:4004–4015.

Richter, R., 2007, *Atmospheric and Topographic Correction for Satellite Imagery: Atcor-2/3 User Guide,Version 6.3*, Köln, Germany: DLR-German Aerospace Centre and Remote Sensing Data Centre, 134 p.

Rodriguez, E., Morris, C. S., Belz, J. E., Chapin, E. C., Martin, J. M., Daffer, W., and S. Hensley, 2005, *An Assessment of the SRTM Topographic Products*, Pasadena, CA: Jet Propulsion Laboratory, Technical Report JPL D-31639, 143 pp.

Steel R. G., Torrie, J. H., and D. A. Dickey, 1997, *Principles and Procedures of Statistics. A Biometrical Approach*, 3rd edition, New York, NY: McGraw-Hill, 665 p.

Sefercik, U. G. and K. Jacobsen, 2007, "Quality Assessment of INSAR Digital Elevation Models," in *27th EARSeL Symposium: "Geoinformation in Europe"*, Bolzano, Italy, June 4–7.

Sun, G., Ranson, K. J., Kharuk, V. I., and K. Kovacs, 2003, "Validation of Surface Height from Shuttle Radar Topography Mission Using Shuttle Laser Altimeter," *Remote Sensing of Environment*, 88(4):401–411

Toutin, T., 1995, "Multi-source Data Fusion with an Integrated and Unified Geometric Modelling," *EARSeL Advances in Remote Sensing*, 4:118–129.

Toutin, T., 2008, "ASTER DEMs for Geomatic and Geoscientific Applications: A Review," *International Journal of Remote Sensing*, 29(7):1855–1875.

U.S. Geological Survey, National Mapping Division, 1998, "Standards for Digital Elevation Models" [http://rockyweb.cr.usgs.gov/nmpstds/acrodocs/dem/2DEM0198 .PDF].

Van Niel, T. G., McVicar, T. R., Li, L., Gallant, J. C., and Q. Yang, 2008, "The Impact of Misregistration on SRTM and DEM Image Differences," *Remote Sensing of Environment*, 112:2430–2442.